Ab initio calculation of the thermodynamic properties and atomic temperature factors of SiO_2 α-quartz and stishovite

Changyol Lee*
Laboratory of Atomic and Solid State Physics, Cornell University, Ithaca, New York 14853-2501

Xavier Gonze
Unité de Physico-Chimie et de Physique des Matériaux, Université Catholique de Louvain, B-1348 Louvain-la-Neuve, Belgium
(Received 29 August 1994; revised manuscript received 28 November 1994)

The constant-volume specific heat, the entropy, the phonon contributions to internal energy and Helmholtz free energy, and the atomic temperature factors of α-quartz and stishovite, two allotropic forms of SiO_2, are calculated as a function of temperature from *ab initio* phonon band structures. Available experimental data agree with our calculated values over a wide range of temperature. α-quartz has more accessible phonon states at low temperatures, while stishovite has larger contributions to the thermodynamic functions from the zero-point motion.

The thermodynamic functions of a solid are determined mostly by the vibrational degrees of freedom of the lattice, since, generally speaking, the electronic degrees of freedom play a noticeable role only for metals at very low temperatures.[1] However, complete knowledge of the vibrational spectrum, with sufficient accuracy, is required for the calculation of these thermodynamic functions. There have been a few early theoretical investigations[2–4] of the thermodynamic properties of SiO_2 α-quartz and stishovite based on models of interatomic forces[5,6] within the harmonic approximation. Predicted phonon density of states and thermodynamic functions from the phonon band structure were of limited accuracy.

We obtained accurate *ab initio* interatomic force constants and phonon band structures of α-quartz and stishovite in our earlier work,[7,8] based on variational density-functional perturbation theory.[9] Therefore, we are now able to calculate *ab initio* thermodynamic functions of α-quartz and stishovite from the phonon band structures, within the harmonic approximation. We will focus on the Helmholtz free energy, the internal energy, the constant-volume specific heat, and the entropy as a function of temperature. Also, knowledge of interatomic force constants allows us to calculate the atomic temperature factors of the atoms, which describe the attenuation of x-ray-diffraction intensities due to the thermal motion of the atoms. A wealth of information on these atomic temperature factors, gathered by crystallographers, is available. Thus, in this Brief Report, we present our calculated thermodynamic quantities and atomic temperature factors, and compare them with the available experimental data.

The above-mentioned thermodynamic functions require summations over phonon eigenstates labeled by the phonon wave vector $\mathbf{q}$ and the phonon mode l. However, the expressions f to be evaluated at each $\mathbf{q}$ and l often depend on $\mathbf{q}$ and l only through the frequency $\omega = \omega(\mathbf{q}, l)$. We can then turn $\sum_{\mathbf{q},l} f(\omega(\mathbf{q}, l))$ into a one-dimensional integral $3nN \int_0^{\omega_L} f(\omega) g(\omega) d\omega$, where n is the number of atoms per unit cell, N is the number of unit cells, ω_L is the largest phonon frequency, and $g(\omega)d\omega$ is defined to be the fractional number of phonon frequencies in the range between ω and $\omega + d\omega$. We normalize the phonon density of states $g(\omega)$ so that $\int_0^{\omega_L} g(\omega) d\omega = 1$, namely, $g(\omega) = (1/3nN) \sum_{\mathbf{q},l} \delta(\omega - \omega(\mathbf{q}, l))$. Specifically, the phonon contribution to the Helmholtz free energy ΔF, the phonon contribution to the internal energy ΔE, as well as the constant-volume specific heat C_v, and the entropy S, at temperature T have the following expressions within the harmonic approximation:[10]

$$\Delta F = 3nNk_BT \int_0^{\omega_L} \ln\left\{2\sinh\frac{\hbar\omega}{2k_BT}\right\} g(\omega)d\omega \ , \tag{1}$$

$$\Delta E = 3nN\frac{\hbar}{2} \int_0^{\omega_L} \omega \coth\left(\frac{\hbar\omega}{2k_BT}\right) g(\omega)d\omega \ , \tag{2}$$

$$C_v = 3nNk_B \int_0^{\omega_L} \left(\frac{\hbar\omega}{2k_BT}\right)^2 \mathrm{csch}^2\left(\frac{\hbar\omega}{2k_BT}\right) g(\omega)d\omega \ , \tag{3}$$

$$S = 3nNk_B \int_0^{\omega_L} \left[\frac{\hbar\omega}{2k_BT}\coth\frac{\hbar\omega}{2k_BT} - \ln\left\{2\sinh\frac{\hbar\omega}{2k_BT}\right\}\right] \times g(\omega)d\omega \ , \tag{4}$$

where k_B is the Boltzmann constant.

The intensity of diffraction from a crystal also depends on temperature, because of the thermal vibrations of the constituent atoms. If the atoms occupied definite positions in the crystal, the intensity of diffraction would be proportional to the square of the structure factor F defined as $\sum_\kappa f_\kappa e^{2\pi i \mathbf{G}\cdot\mathbf{r}_\kappa}$, where f_κ is the scattering amplitude of the atom κ, $\mathbf{G}$ is the scattering wave vector, and $\mathbf{r}_\kappa$ is the position of the atom κ. The diffraction condition requires $\mathbf{G}$ to be a reciprocal lattice vector. At finite temperature, the atoms oscillate around their equilibrium positions and the structure factor is modified as $F_T = \sum_\kappa f_\kappa e^{-W(\kappa)} e^{2\pi i \mathbf{G}\cdot\mathbf{r}_\kappa}$ where the atomic temperature factor $e^{-W(\kappa)}$ at temperature T is defined[11] as

$$e^{-W(\kappa)} = \exp\left(-\frac{1}{2}\sum_{ij} B_{ij}(\kappa) G_i G_j\right) \ , \tag{5}$$

with the mean-square displacement matrix $B_{ij}(\kappa)$ given by

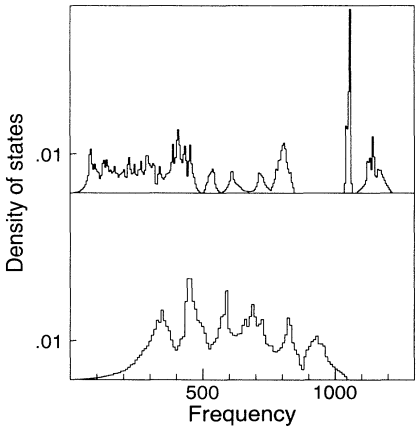

FIG. 1. The phonon densities of states $g(\omega)$ of α-quartz (upper panel) and stishovite (lower panel). $\int g(\omega)d\omega = 1$ and the frequencies are in cm^{-1}.

$$B_{ij}(\kappa) = \frac{1}{N}\sum_{\mathbf{q},l} \frac{\hbar}{2\omega(\mathbf{q},l)} \coth\frac{\hbar\omega(\mathbf{q},l)}{2k_BT} e_i(\kappa|\mathbf{q},l)e_j^*(\kappa|\mathbf{q},l) \ , \tag{6}$$

where M_κ is the mass of the atom κ, G_i is the ith component of the scattering wave vector $\mathbf{G}$, and $e_i(\kappa|\mathbf{q},l)$ is the ith component of the displacement eigenvector associated with the atom κ and the mode l at $\mathbf{q}$ in the Cartesian coordinates, normalized such that $\sum_l M_\kappa e_i(\kappa|\mathbf{q},l)e_j^*(\kappa'|\mathbf{q},l) = \delta_{ij}\delta_{\kappa\kappa'}$. When there is only one kind of atom with sufficient local symmetry, all the $e^{-W(\kappa)}$ are identical and $|F_T|^2 = |F|^2e^{-2W(\kappa)}$. In this case, the intensity of diffraction is reduced by a factor of $e^{-2W(\kappa)}$, which is usually called the Debye-Waller factor. For two or more kinds of atoms, there is no simple relation between $|F|^2$ and $|F_T|^2$. From Eq. (6), one can see that $e^{-W(\kappa)}$ and $B_{ij}(\kappa)$ cannot be calculated from $g(\omega)$ due to the explicit dependence on eigenvectors. However, it is efficient to express $B_{ij}(\kappa)$ in terms of "generalized" density of states $g_{ij}(\kappa|\omega)$ as follows:

$$B_{ij}(\kappa) = \frac{1}{M_\kappa}\int_0^{\omega_L} \frac{\hbar}{2\omega} \coth\left(\frac{\hbar\omega}{2k_BT}\right) g_{ij}(\kappa|\omega)d\omega, \tag{7}$$

where $g_{ij}(\kappa|\omega)$ is defined as

$$g_{ij}(\kappa|\omega) = \frac{1}{N}\sum_{\mathbf{q},l} M_\kappa e_i(\kappa|\mathbf{q},l)e_j^*(\kappa|\mathbf{q},l)\delta(\omega - \omega(\mathbf{q},l)) \ . \tag{8}$$

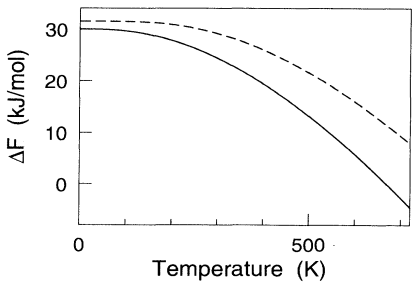

FIG. 2. The phonon contribution to the Helmholtz free energies ΔF of α-quartz (solid line) and stishovite (dashed line).

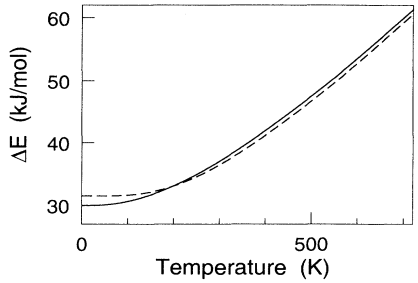

FIG. 3. The phonon contribution to the internal energies ΔE of α-quartz (solid line) and stishovite (dashed line).

The generalized density of states $g_{ij}(\kappa|\omega)$ has to be calculated only once for each atom κ and is normalized in such a way that $\int_0^{\omega_L} g_{ij}(\kappa|\omega)d\omega = \delta_{ij}$ for each atom κ.

We use the root sampling (or histogram) method[10] on the phonon wave vectors $\mathbf{q}$ for the calculations of the phonon densities of states $g(\omega)$ and generalized densities of states $g_{ij}(\kappa|\omega)$. We then calculate the thermodynamic functions and the mean-square displacement matrix using Eqs. (1)–(4) and (7), with the rectangular formula for integration from the functional values at the midpoint of each frequency channel. At the low-frequency limit, the factors multiplying the densities of states show logarithmic divergence in Eqs. (1) and (4) and quadratic divergence in Eq. (7). However, since the density of states and generalized density of states both behave as the square of frequency at the low-frequency limit, the actual integrands behave regularly, approaching zero in Eqs. (1) and (4) and a constant in Eq. (7). Therefore, it is possible to check the convergence of the contribution from each rectangular channel in our integration scheme by decreasing the width of the frequency channel. We first fix the width of the frequency channel and increase the resolution of the homogeneous sampling of the phonon wave vectors in the Brillouin zone until each channel of the density of states converges within a preassigned accuracy. Then we repeat the same procedure with a smaller width of the frequency channel until the convergence of the thermodynamical quantities and the mean-square displacement matrix is obtained. In order to get the mean of the relative error in each channel of the phonon densities of states smaller than 2%, and the thermodynamical quantities and the mean-square displacement matrix elements converged to better than 0.1% and 1%, respectively, at all temperatures studied, we find it sufficient to sample the

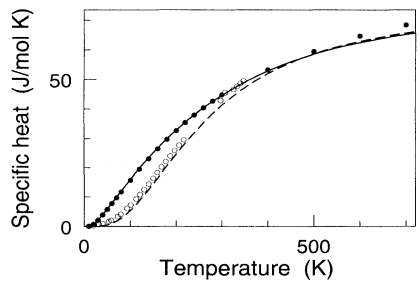

FIG. 4. The constant-volume specific heats of α-quartz (calculated values in the solid line; solid circles, experimental data from Ref. 3) and stishovite (calculated values in the dashed line; open circles, experimental data from Ref. 13).

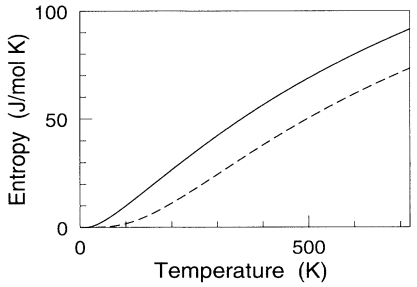

FIG. 5. The entropy of α-quartz (solid line) and stishovite (dashed line).

phonon wave vectors $\mathbf{q}$ from (60,60,40) Monkhorst-Pack grids[12] with channel width 5 cm^{-1} for the thermodynamic functions of α-quartz, from (45,45,30) grids with channel width 9 cm^{-1} for the mean-square displacement matrix elements of α-quartz, from (40,40,80) grids with channel width 9 cm^{-1} for the thermodynamic functions of stishovite, and from (50,50,100) grids with channel width 9 cm^{-1} for the mean-square displacement matrix elements of stishovite, respectively.

In Fig. 1, the phonon densities of states of α-quartz and stishovite are shown. We observe that the two densities of states are quite different: α-quartz has more complex structure with a very high peak at around 1060 cm^{-1}, a wide gap between 846 and 1038 cm^{-1}, and the largest frequency 1218 cm^{-1}, whereas stishovite has a continuous distribution and the largest frequency 1050 cm^{-1}. α-quartz has a significant density at low frequencies, while stishovite has a low density until the first peak (around 350 cm^{-1}) is reached. The stishovite lattice could be characterized as more rigid than the α-quartz lattice, if it were not for the presence of the large frequency modes, beyond 1050 cm^{-1}. The latter modes can be associated with the breathing and distortion of the tetrahedral building blocks SiO_4 of α-quartz. Due to the fact that at low temperature more phonon states are available in α-quartz than in stishovite, a difference is expected in the thermodynamic functions.

The temperature-dependent phonon contributions ΔF and ΔE to the Helmholtz free energy F (see Fig. 2) and the internal energy E (see Fig. 3) are calculated from the phonon densities of states. The zero-temperature values ΔF_0 and ΔE_0 do not vanish, due to the zero-point motion, and can be calculated from the asymptotic expressions of Eqs. (1) and (2):

$$\Delta F_0 = \Delta E_0 = 3nN \int_0^{\omega_L} \frac{\hbar\omega}{2} g(\omega) d\omega \ . \tag{9}$$

We find $\Delta F_0 = \Delta E_0 = 30.0$ kJ/mol for α-quartz and 31.5 kJ/mol for stishovite. The temperature-dependent ΔE is higher for stishovite between 0 and 200 K and higher for α-quartz above 200 K, whereas ΔF is higher for stishovite at all temperature due to the lower entropy of the more rigid structure of stishovite. Note that the harmonic approximation will break down for α-quartz as soon as the temperature approaches 846 K, where a second-order phase transition to β-quartz takes place.

Next, the constant-volume specific heats C_v are calculated and compared to the experimental data from Refs. 3, 13. The agreement between our calculated specific heats and the experimental data is excellent as shown in Fig. 4. The discrepancies between the calculated and experimental specific heats become larger at high temperature as the lattice undergoes thermal expansion due to the anharmonic interactions. Stishovite has lower specific heat than α-quartz at temperature below 480 K and the specific heats of α-quartz and stishovite are very close above 480 K. Also, the two specific heats approach at high temperatures the classical asymptotic

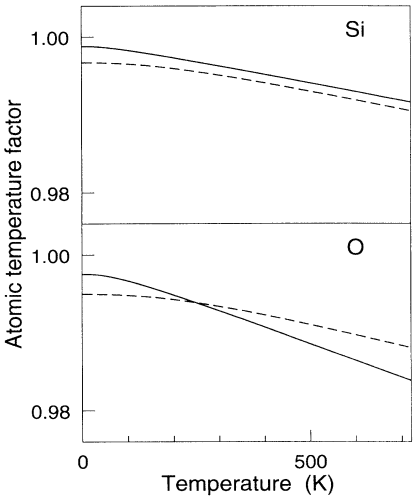

FIG. 6. The atomic temperature factors of Si and O atoms in α-quartz (solid line) and stishovite (dashed line) for the diffraction with scattering vector $\mathbf{G} = (2\pi/c)\,\hat{\mathbf{z}}$.

TABLE I. The thermal parameter β_{ij} of Si and O atoms in α-quartz at room temperature.

	Atom	β_{11} (Å^2)	β_{22} (Å^2)	β_{33} (Å^2)	β_{12} (Å^2)	β_{13} (Å^2)	β_{23} (Å^2)
This work	Si	0.0070	0.0055	0.0054	$\frac{1}{2}\beta_{22}$	$\frac{1}{2}\beta_{23}$	−0.0004
Ref. 14	Si	0.0045	0.0025	0.0072	$\frac{1}{2}\beta_{22}$	$\frac{1}{2}\beta_{23}$	−0.0002
Ref. 15	Si	0.0048	0.0027	0.0063	$\frac{1}{2}\beta_{22}$	$\frac{1}{2}\beta_{23}$	0.0004
Ref. 16	Si	0.0065	0.0054	0.0059	$\frac{1}{2}\beta_{22}$	$\frac{1}{2}\beta_{23}$	−0.0002
Ref. 17	Si	0.0066	0.0051	0.0060	$\frac{1}{2}\beta_{22}$	$\frac{1}{2}\beta_{23}$	−0.0003
Ref. 18	Si	0.0085	0.0072	0.0073	$\frac{1}{2}\beta_{22}$	$\frac{1}{2}\beta_{23}$	−0.0002
This work	O	0.0155	0.0109	0.0103	0.0090	−0.0033	−0.0042
Ref. 14	O	0.0131	0.0074	0.0133	0.0078	−0.0037	−0.0049
Ref. 15	O	0.0128	0.0105	0.0128	0.0069	−0.0035	−0.0044
Ref. 16	O	0.0163	0.0127	0.0128	0.0097	−0.0027	−0.0043
Ref. 17	O	0.0156	0.0115	0.0119	0.0092	−0.0029	−0.0046
Ref. 18	O	0.0174	0.0132	0.0123	0.0097	−0.0029	−0.0041

TABLE II. The thermal parameter $\beta_{ij}(\kappa)$ of Si and O atoms in stishovite at room temperature.

	Atom	β_{11} (Å^2)	β_{22} (Å^2)	β_{33} (Å^2)	β_{12} (Å^2)	β_{13} (Å^2)	β_{23} (Å^2)
This work	Si	0.00228	β_{11}	0.00177	0.00007	0	0
Ref. 19	Si	0.00253	β_{11}	0.00196	0.00014	0	0
Ref. 20	Si	0.00236	β_{11}	0.00178	0.00016	0	0
This work	O	0.00301	β_{11}	0.00238	−0.00082	0	0
Ref. 19	O	0.00327	β_{11}	0.00248	−0.00095	0	0
Ref. 20	O	0.00308	β_{11}	0.00231	−0.00084	0	0

limit of 74.8 J/mol K.

The entropies are also calculated (see Fig. 5). Stishovite is found to have lower entropy than α-quartz over the entire temperature range, due to its smaller density of states for low-frequency modes.

Finally, the mean-square displacement matrix elements $B_{ij}(\kappa)$ for Si and O atoms in α-quartz and stishovite are calculated as a function of temperature. Crystallographers, however, often provide the thermal parameters $\beta_{ij}(\kappa)$ which are the mean-square displacements of the atom κ along the *crystal* axes i and j. Therefore, we convert the mean-square displacement matrix $B_{ij}(\kappa)$ into the thermal parameters $\beta_{ij}(\kappa)$ for comparison. Due to the symmetry of the crystal structure, $\beta_{22}(\mathrm{Si}) = 2\beta_{12}(\mathrm{Si})$ and $\beta_{23}(\mathrm{Si}) = 2\beta_{13}(\mathrm{Si})$ in α-quartz, and $\beta_{11}(\kappa) = \beta_{22}(\kappa)$ and $\beta_{13}(\kappa) = \beta_{23}(\kappa) = 0$ for $\kappa =$ Si or O in stishovite. Experimental values, obtained from analysis of raw data through model calculations, show large discrepancies between each other. Our calculated values show reasonable agreement with these results (see Tables I and II). The sole large systematic discrepancy, over 10%, is found for the β_{33} element in α-quartz. This discrepancy could be due to the anharmonicity of the interatomic potential. Experimental uncertainties likely preclude the observation of this effect for the other components of the β tensor in α-quartz, while stishovite is a less anharmonic material than α-quartz. The typical mean-square displacements of Si and O atoms in stishovite are rather similar (between 0.001 77 and 0.003 01 Å^2), while the mean-square displacement of the Si atoms in α-quartz is roughly 3 times larger than this value (0.0054 and 0.0070 Å^2), and the β_{11} component of the O atoms reaches up to 0.0155 Å^2. The smaller displacements in stishovite are a consequence of the rigidity of its lattice. The atomic temperature factors $e^{-W(\kappa)}$ are also calculated as a function of temperature for the diffraction with scattering vector $\mathbf{G} = (2\pi/c)\,\hat{\mathbf{z}}$ (see Fig. 6). $e^{-W(\kappa)}$ is not 1 even at 0 K due to the zero-point motion. The O atoms in α-quartz, having large values of the mean-square displacements, show a larger change in the atomic temperature factor as a function of temperature than the Si atoms in α-quartz and the Si or O atoms in stishovite.

In conclusion, we have calculated the thermodynamic functions of SiO_2 α-quartz and stishovite as a function of temperature from *ab initio* phonon band structures. We find excellent agreement between our calculated specific heat and the experimental data. The zero-point motion contribution to the thermodynamic functions of stishovite is more important than the one of α-quartz. Due to the difference in the structures of the phonon densities of states for α-quartz and stishovite, i.e., more low-frequency distributions for α-quartz than stishovite, the thermal vibrations become more important for α-quartz as the temperature increases from 0 K. Therefore, the phonon contribution to the internal energies is larger in stishovite than in quartz at low temperature, but smaller at high temperature. The atomic temperature factor of the O atoms in α-quartz shows a larger change than the Si atoms in α-quartz and the Si or O atoms in stishovite.

We acknowledge stimulating discussions with Professor R.O. Pohl, Dr. S. Kiselev, and Dr. D.C. Allan. This work is supported by the Cornell Theory Center and Corning Incorporated (C.L.) and FNRS-Belgium (X.G.).

* Present address: Battelle Memorial Institute, Pacific Northwest Laboratory, Richland, WA 99352.

[1] L. D. Landau and E. M. Lifshitz, *Statistical Physics,* 3rd. ed. (Pergamon, London, 1980), Pt. 1, p. 193.
[2] B. D. Saksena, Proc. Indian Acad. Sci. **12A**, 93 (1940).
[3] R. C. Lord and J. C. Morrow, J. Chem. Phys. **26**, 230 (1957).
[4] M. E. Striefler and G. R. Barsch, Phys. Rev. B **12**, 4553 (1975).
[5] M. M. Elcombe, Proc. Phys. Soc. London **91**, 947 (1967).
[6] S. W. Kieffer, Rev. Geophys. Space Phys. **17**, 20 (1979).
[7] C. Lee and X. Gonze, Phys. Rev. Lett. **72**, 1686 (1994).
[8] X. Gonze *et al.*, Phys. Rev. B **50**, 13035 (1994).
[9] X. Gonze *et al.*, Phys. Rev. Lett. **68**, 3603 (1992); X. Gonze (unpublished).
[10] A. A. Maradudin *et al.*, in *Solid State Physics*, 2nd ed., edited by H. E. Ehrenreich *et al.* (Academic, New York, 1971), Chap. 4.
[11] B. T. M. Willis and A. W. Pryor, *Thermal Vibrations in Crystallography* (Cambridge University Press, Cambridge, England, 1975).
[12] H. J. Monkhorst and J. D. Pack, Phys. Rev. B **13**, 5188 (1976).
[13] J. L. Holm *et al.*, Geochim. Cosmochim. Acta **31**, 2289 (1967).
[14] R. A. Young and B. Post, Acta Crystallogr. **15**, 337 (1962).
[15] G. S. Smith and L. E. Alexander, Acta Crystallogr. **16**, 462 (1963).
[16] W. H. Zachariasen and H. A. Plettinger, Acta Crystallogr. **18**, 710 (1965).
[17] Y. Le Page and G. Donnay, Acta Crystallogr. B **32**, 2456 (1976).
[18] L. Levien *et al.*, Am. Mineral. **65**, 920 (1980).
[19] R. J. Hill *et al.*, J. Solid State Chem. **47**, 185 (1983).
[20] M. A. Spackman *et al.*, Phys. Chem. Miner. **14**, 139 (1987).